Composites Part A 119 (2019) 38–47

Contents lists available at ScienceDirect

Composites Part A

journal homepage: www.elsevier.com/locate/compositesa

Investigating the effects of fiber surface treatment and alignment on mechanical properties of recycled carbon fiber composites

Nekoda van de Werken[a], Malcolm S. Reese[a], Mahmoud R. Taha[b], Mehran Tehrani[a,*]

[a] Advanced Structural and Energy Materials Laboratory, Department of Mechanical Engineering, University of New Mexico, Albuquerque, NM, United States
[b] Department of Civil, Construction & Environmental Engineering, University of New Mexico, Albuquerque, NM, United States

ARTICLE INFO

Keywords:
Recycled carbon fibers
Fiber alignment
Mechanical properties
Analytical modeling

ABSTRACT

Recycled carbon fibers cost a fraction of virgin fibers and their composites can potentially achieve mechanical properties suitable for a wide range of applications. When recycled, carbon fibers usually become millimeter to centimeter long and emerge as a tangled mass analogous to cotton candy. In this work, recycled carbon fibers were processed into unidirectionally aligned and two-dimensional randomly oriented recycled carbon fiber mats. The surface of the recycled carbon fibers was probed to understand the significance of surface characteristics on the mechanical behavior of recycled carbon fiber composites. Tensile testing was used to determine the influence of fiber surface quality, aspect ratio, and alignment on mechanical properties of the composites. It is concluded that the processing has a significant effect on the properties of recycled fiber composites. An analytical model was validated and subsequently used to provide insight into viable methods for improving mechanical properties in recycled carbon fiber composites.

1. Introduction

Carbon fiber reinforced polymer composites (CFRPs) exhibit unique combination of properties, such as low density, high strength and stiffness, corrosion resistance, fatigue resistance, and controllable anisotropic mechanical properties [1]. This combination of properties has led to the utilization of CFRPs in a diverse set of markets, such as wind energy, aerospace, infrastructure, high end cars, and luxury sport equipment [2]. However, the high cost associated with carbon fiber composites has limited their applications to mostly aerospace industries and been a major barrier for their widespread adoption into other large volume markets such as the automotive [2]. Recycled carbon fibers have recently emerged as an inexpensive and environmentally friendly alternative with attractive mechanical performance.

The production of virgin carbon fiber is an energy intensive process, requiring 50–150 kWh/kg. Such a production process together with the high cost of carbon fiber precursor dictates the high price of carbon fibers [3]. Naturally, this high cost has placed a premium on high-performance alternatives to virgin carbon fiber. One alternative is recycled carbon fibers, which can be produced at a fraction of the cost while maintaining nearly all the mechanical properties of the virgin fibers [4,5]. Carbon fibers can be reclaimed from end-of-life composites at an energy cost as low as 3–9 kWh/kg, which significantly reduces the price compared with virgin carbon fibers [6]. The use of recycled carbon fiber is environmentally attractive, potentially reducing greenhouse gases for producing new carbon fibers and diverting composite waste from landfills and incineration, which are the current most common disposal methods for end-of-life carbon fiber composites [7].

Carbon fiber reclamation has been accomplished through pyrolysis, solvolysis, and a fluidized bed process, each with its own advantages and limitations [4]. Pyrolysis recovers fiber reinforcement from a composite by burning off the polymer matrix at elevated temperatures [4]. Chemical recycling can produce fibers with very high retention of mechanical properties, though the process may not be robust to contamination [4]. The fluidized bed process is robust to many types of contamination and has been well documented, though degradation of the fiber length and properties have been reported [4,8,9].

Nahil et al. investigated the use of pyrolysis to recycle a carbon fiber polybenzoxazine composite in a fixed bed reactor, which produced fibers with 90% of virgin fiber mechanical properties [10]. Jiang et al. studied the contact angles and interfacial bonding of carbon fibers recycled via pyrolysis, finding that T800 carbon fibers had reduced wetting and lower interfacial shear strength with thermosetting resins than virgin T800 fibers [11]. Jiang et al. also found that pyrolysis recycling results in both a decrease in fiber strength and fiber-epoxy interfacial shear strength [12]. The fibers experienced a reduction in lateral crystallite size on their surface, along with an expansion between graphitic layers. The 2–16% reduction in fiber tensile strength is

* Corresponding author.
E-mail address: mtehrani@unm.edu (M. Tehrani).

https://doi.org/10.1016/j.compositesa.2019.01.012
Received 22 October 2018; Received in revised form 31 December 2018; Accepted 15 January 2019
Available online 16 January 2019
1359-835X/

thought to be related to surface defects introduced in the process, while the 24% reduction in interfacial shear strength (IFSS) is related to a 2.6–42% decrease in surface oxygen concentration [12].

Catalytic recycling processes at relatively low temperatures but high pressures can also produce fibers with 83–99% virgin strength and varying degrees of surface oxidation [13]. Moreover, supercritical and near-supercritical water with the addition of a potassium hydroxide catalyst can be used to remove up to 95.3 wt% of epoxy from a composite [14]. These recycled fibers retained between 90% and 98% of the virgin fiber tensile strength. The use of supercritical n-propanol to reclaim carbon fibers was studied further in 2009. It was found that while the vast majority of resin was removed, the fiber surface experienced a decrease in C—OH groups [15]. This decrease is likely responsible for the reduction in IFSS between the fibers and epoxy. While most recycling technologies retain 80–100% of the fiber level mechanical properties, fiber surfaces and their interactions with polymers usually deteriorate.

Various re-manufacturing methods have been developed for recycled carbon fiber composites (rCFRP). Many methods are borrowed from discontinuous fiber composites and applied to rCFRPs. These processes typically produce uniformly aligned or randomly oriented composites. Randomly aligned composites reduce the cost of re-manufacturing but observe a corresponding reduction in achievable volume fraction and mechanical properties. An overview of aligned short fiber composites was provided by Such et al. in 2014 [16], beginning with the first instances of fiber alignment methods developed in the early 1960s.

In 2010, Turner et al. outlined a portion of the challenges facing recycled carbon fiber composite technology, concluding that fiber alignment would be a critical factor in producing competitive recycled fiber composites [17]. Turner et al. produced an aligned recycled carbon fiber composite with a 44% volume fraction and a strength and modulus of 422 MPa and 80 GPa, respectively, using compression molding with 5–10 MPa molding pressure [17]. In 2014, Yu et al. developed the High Performance-Discontinuous Fiber (HiPerDiF) alignment method [18]. This method was used to successfully align 67% of 3 mm long tape type preforms from virgin carbon fibers within the range of ± 3°. The composite made from these aligned fibers had a volume fraction of 55%, with a strength and stiffness of 1509 MPa and 115 GPa, respectively [18]. While this technique may be applicable to recycled carbon fibers, the alignment of recycled carbon fibers was not considered in this study.

The potential benefits of recycled carbon fiber composites have become apparent, though further work is needed to bring the technology into large-scale markets. The focus of this study is on investigating the effect of sizing, processing, and alignment on the mechanical properties of rCFRP composites. Sized and non-sized fibers were used to make composites with either uni-directionally aligned fiber mats or 2D randomly oriented fiber mats. The fiber mats were then infused with epoxy using a resin transfer molder. The individual fibers and composites were characterized and an analytical model was used to contextualize the observed properties and prescribe directions for designing recycled carbon fiber composites for different applications. The validated model of the rCFRP was used to understand the effects of fiber aspect ratio, alignment, and interfacial strength on the mechanical properties of rCFRP composites.

2. Materials and methods

2.1. Materials

Toray T800 carbon fiber epoxy composites were recycled by Adherent Technologies Inc. using a wet chemical process. Adherent Technologies Inc. combines a catalyst-based wet recycling process with vacuum pyrolysis treatment to successfully reclaim 99% clean carbon fibers [19]. The wet recycling process is performed at low temperatures inside of a low pressure vessel (150 °C and 150 psi) to fully recover carbon fibers while causing minimal damage to their surface [20]. A proprietary epoxy-based sizing agent was applied to a selection of the recycled fibers, and both as-is and sized fibers were used to make composite plates. The fiber length ranged from ~10 to 50 mm, and the fibers were received in a highly entangled fluffy architecture, as shown in Fig. 1. A 95 wt% glycerol/water solution was used to disperse the recycled fibers using an axial impeller. Aeropoxy PR2032 resin and PH3660 hardener (100:27 wt/wt) were used as the epoxy system for the composite plates. Following our previous studies, the Aeropoxy was cured at room temperature for 18 h, followed by a two-hour post-cure at 80 °C [1,21,22].

Fig. 1. As-received recycled carbon fibers resemble cotton candy of highly entangled fibers.

2.2. Scanning electron microscopy

Scanning electron microscopy (SEM) micrographs were collected using an FEI Quanta 3D FEG SEM. Samples were prepared by fixing a random selection of fibers to the sample holder using electrically conductive carbon tape. The micrographs were used to characterize the surface quality and diameter of the as-received sized and non-sized carbon fibers. The features of interest were defects such as pitting or residual epoxy, or foreign contaminants that may have been introduced to the recycling process.

2.3. X-ray photoelectron spectroscopy

The active chemical groups on the fiber surface before and after sizing and after the mat remanufacturing processing were analyzed with a Kratos AXIS Ultra X-ray photoelectron spectrometer (XPS). The spectrometer was equipped with a monochromatic Al Kα source operating at 300 W, with a base pressure of 2×10^{-10} torr and an operating pressure of 2×10^{-9} torr. High-resolution spectra were taken of the C1s, N1s, and O1s peaks at 20 eV.

2.4. Single fiber tensile test

The mechanical properties of the individual recycled carbon fibers were characterized using single fiber tensile tests. The tests were performed with a DMA Q800 equipped with film tension clamps, following the ASTM C1557-14 standard. Single carbon fibers were placed across a 12.7 mm square window in a piece of card stock. The ends of the fibers were glued to the paper with a cyanoacrylate adhesive. The samples were mounted in the clamps, and the sides of the paper were cut away to leave only the single fiber between the two clamps. The test was carried out at a displacement rate of 20 μm/s until fiber failure.

A Weibull analysis was applied to the single fiber tensile data results [23]. For this study, 20 fibers were tested. A least squares regression fit was used with this data to find the shape and scale parameters. The scale parameter is used to identify the stress at which the weakest 63%

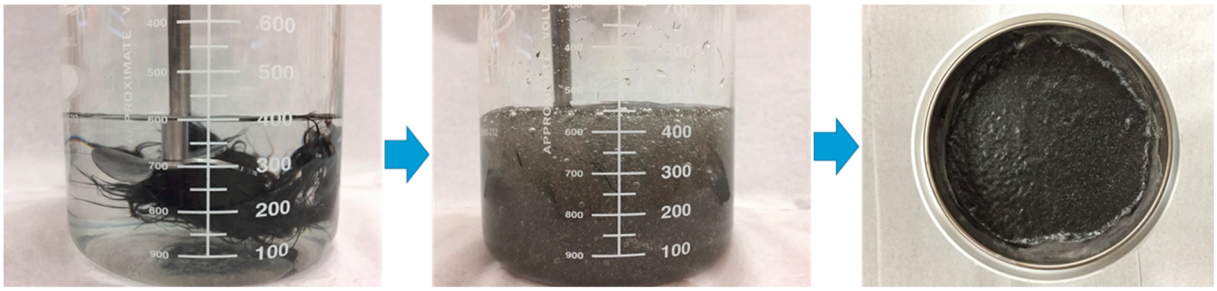

Fig. 2. Non-aligned mat production process involving dispersion of recycled fibers into a viscous glycerol solution and deposition of fibers onto a nylon-covered sieve. (For interpretation of the references to colour in this figure legend, the reader is referred to the web version of this article.)

of fibers in a population will fail and thus acts as an appropriate metric to compare the strengths of different samples [15].

2.5. rCF mat fabrication

Randomly oriented 2D fiber mats were fabricated using a vacuum filtration method, as illustrated in Fig. 2. A carbon fiber slurry was created by dispersing the recycled fiber bundles in a viscous glycerol solution using an axial impeller. The high viscosity allows for larger shear forces to be imparted on the fiber bundles, assisting in the dispersion to the single-fiber level. Roughly 500 mg of fibers were dispersed in 200–400 ml of glycerol/water solution. The axial impeller was run at 1100 rpm in five-minute intervals. After five minutes, any remaining fiber bundles were removed from the solution, and the dispersed fiber slurry was poured uniformly onto a nylon mesh covering a 10 cm stainless steel sieve. Vacuum was applied to remove glycerol and densify the fiber mat. The five-minute mixing time was designed to prevent excess damage to the fibers. Undispersed fiber bundles were added to the clean glycerol for the subsequent mixing step. This process was repeated until ~10 g of fibers were deposited on the mat. The mat was then thoroughly rinsed with warm DI water to remove glycerol and dried at 180 °C for two hours. Reference samples based on virgin T800 fibers were also processed into mats.

A lower concentration of carbon fibers in the slurry was necessary to achieve highly aligned carbon fiber mats. The carbon fiber slurry was prepared by adding approximately 60–100 mg of carbon fiber to 500 ml of the glycerol solution. This solution was mixed with the axial impeller at 1100 rpm for 5 min before an additional 60–100 mg of fibers were added. The impeller was placed near the edge of the mixing container, in this case a one-liter funnel, to maximize shear forces in the region between the impeller and container wall. Within the funnel, larger bundles of fibers were trapped in the fluid vortex while dispersed fibers travelled with the glycerol out of the funnel.

When the fiber slurry exited the funnel, it travelled through a flexible tube toward a convergent nozzle. The tube and nozzle were attached to a reciprocating rack, which travelled on a single axis according to an alternating and constant positive and negative velocity over a 6 cm distance. The convergent nozzle was positioned inside of a rotating mesh drum, with the nozzle exit velocity aligned tangentially to the drum circumference. The fibers become partially aligned in the convergent nozzle and are further aligned as they contact the mesh on the drum. The difference in velocity between the fiber slurry jet and drum rotation causes the bottom of the fiber to be 'pulled' along the circumference of the drum to encourage alignment in that direction. A schematic of the alignment rig and an example of an aligned mat produced with this technique is illustrated in Fig. 3. Mats were finally rinsed with warm deionized (DI) water and dried at either 180 °C or 300 °C. The latter temperature was chosen to ensure evaporation of any remaining glycerol, which evaporates at ~290 °C.

The use of a centrifugal alignment rig to align discontinuous fibers was first developed in 1980 by Edwards and Evans [16], and utilized later by Wong et al. [24]. In this study, the use of a funnel for dispersing

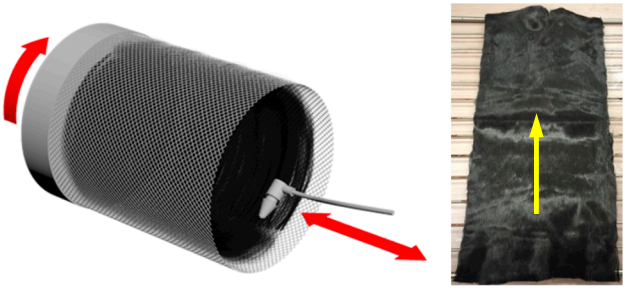

Fig. 3. Centrifugal alignment rig concept and 60 × 120 mm fabricated aligned carbon fiber mat. Red arrows indicate the mechanical motion of the components. The yellow arrow indicates alignment direction. The collection cylinder, typically surrounding this device, is left out for clarity. (For interpretation of the references to colour in this figure legend, the reader is referred to the web version of this article.)

the carbon fibers restricted the entry of fiber bundles from entering the nozzle. The alignment rig used in this study also allowed for control over solution temperature (and consequently viscosity), drum rotation rate, and nozzle linear velocity.

The length, width, and thickness of the resulting aligned carbon fiber mat are determined by the drum diameter, maximum nozzle travel, and the amount of fibers deposited, respectively. The drum was made from a rolled piece of 70 × 150 mm stainless-steel wire cloth, with a 0.8 mm wire diameter and a 1.3 mm opening size (37.5% open area). However, the carbon fibers do not tend to adhere well to the steel, so a thin nylon mesh was inserted to cover the inside of the drum. This also allows for simplified removal of the aligned mat once the desired thickness is achieved. The mat was carefully rinsed and dried once the desired thickness was achieved. Design of experiments was used to find the optimum flow rates and lateral nozzle speeds. A nozzle linear velocity of 2.5 cm/s, temperature of 30 °C, and drum rotational velocity of 600 rpm were found to be most effective at aligning the fiber mat. Additionally, the alignment would decrease as the mat thickness increased and permeability decreased. Therefore, mats were made containing 1g of material and stacked to achieve the desired composite thickness.

2.6. Fiber alignment and length characterization

The alignment was characterized by tracing individual fibers in a micrograph using the software ImageJ. This technique was used to find the respective angle of each fiber in a representative micrograph. From this data, a fiber angle histogram was generated for the front and back of the aligned fiber mat.

To ensure that the processing of carbon fibers into aligned mats did not degrade the fiber length beyond the critical length, the length distribution of fibers was found through image analysis. For this experiment, a random selection of fibers was taken from a processed, rinsed and dried rCF mat and dispersed across a piece of white cardstock. Once

the fibers were dispersed enough to allow for individual length identification, an image was taken of roughly a 50 × 50 mm^2 square area. The fibers were traced with image analysis software (ImageJ) to measure their length. Over 500 fibers were measured with this technique, and a length distribution histogram was generated.

2.7. Resin transfer molding

Resin transfer molding (RTM) was used to fabricate the composite plates for this study. The epoxy was degassed for a minimum of 30 min before being injected into the mold and was infused at a rate of 2 cc/min for 50 min.

2.8. Composite characterization

The tensile properties of the rCFRP specimens were measured following the ASTM D3039/D3039M guidelines. Fiberglass composite tabs were attached to each end of the tensile coupons using Aeropoxy, following the standard degassing, mixing, and curing procedure. The tabs were roughened prior to bonding with 240 grit silicon carbide paper to improve adhesion. The tests were performed with an Instron 4400R, at a constant displacement rate of 1.3 mm/min. The rCFRP specimens were also examined using micro-computed tomography (μCT). This characterization was used to observe the 3D alignment of the fibers within the samples, and monitor voids, defects, and contamination. A Zeiss Xradia 520 Versa was used to collect the data for the samples, and the data was analyzed using Dragonfly Pro.

2.9. Modeling tensile properties of short fiber reinforced composites

Analytical models for the prediction of tensile strength and stiffness of short fiber composites have been developed and validated [25–29]. These models can be used to assess the recycled fiber composites examined in this study, including the Halpin Tsai semi-empirical equations, composite mechanics approach and laminate analogy approach, incorporating the experimentally measured fiber orientation and length distributions of the specimens [25,27]. These analytical models require a precise description of fiber length and orientation distributions, as well as fiber interfacial and tensile strength. Length and orientation distributions can be mathematically described by probability density functions. The probability density function for fiber lengths or fiber length distribution (FLD) is defined such that the probability of fibers with a length between l and $l + dl$ is $f(l)dl$. A similar probability function, $g(\theta)$, can be defined for fiber orientation distribution (FOD) [26,30]. The experimental FLD and FOD were fitted to:

$$f(l) = abl^{b-1}\exp(-al^b) \tag{1}$$

where a and b are parameters that define FLD,

$$g(\theta) = \frac{\sin\theta^{2p-1}\cos\theta^{2q-1}}{\int_{\theta_{min}}^{\theta_{max}} \sin\theta^{2p-1}\cos\theta^{2q-1}d\theta} \tag{2}$$

for $0 \le \theta_{min} \le \theta \le \theta_{max} \le \pi/2$, where p and q are shape parameters that determine the FOD function shape. For example, if $p = q = 0.5$, fibers are randomly distributed and for $p = 0.5$ and $q > 100$, almost all fibers are aligned in the 0° direction.

Experimental FLD and FOD were fit to Eqs. (1) and (2) using the least square method in a Matlab script, as shown in Fig. 4. Fit parameters were found to be $p = 0.51$, $q = 2.2$, $a = 0.285$, and $b = 1.554$.

The strength of partially aligned discontinuous fiber composite can be estimated using a mechanics approach [30]. Interfacial shear stress between fiber and matrix increases with increasing the applied load. Strength of the composite can be estimated by evaluating the average stress required to break the composite at some random cross section. For a single fiber that intersects a crack at an angle, θ:

$$\sigma_{F\theta} = \sigma_F[1 - A_f\tan(\theta)] \tag{3}$$

where A_f is a constant equal to 0.083 for carbon-epoxy systems and σ_F is the strength of fiber when the crack plane is perpendicular to fiber axis [29]. Fiber failure in a composite depends strongly on the critical fiber length. The critical length of an oblique fiber can be written as:

$$l_{c\theta} = \frac{l_c[1 - Af\tan(\theta)]}{\exp(\mu\theta)} \tag{4}$$

where l_c is the critical fiber length for a straight fiber and μ is the snubbing friction and is estimated as 0.1 in our model [30].

The composite strength can then be calculated using the following expression:

$$\sigma_c = \chi_1\chi_2\sigma_F\nu_f + \sigma_M\nu_m \tag{5}$$

$$\begin{aligned}\chi_1\chi_2 = &\int_{\theta_{min}}^{\theta_{max}}\int_{l_{min}}^{l_{c\theta}} f(l)g(\theta)(l/l_{mean})(l/2l_c))\exp(\mu\theta)\mathrm{d}l\mathrm{d}\theta \\ &+ \int_{\theta_{min}}^{\theta_{max}}\int_{l_{c\theta}}^{l_{max}} f(l)g(\theta)(l/l_{mean})(1 - A_f\tan(\theta)) \\ &\times(1 - l_c(1 - A_f\tan(\theta))/(2l\exp(\mu\theta)))dldl\theta\end{aligned} \tag{6}$$

where ν_f is the fiber volume fraction, ν_m is the matrix volume fraction, and χ_1 and χ_2 are fiber orientation factor and fiber length factor, respectively. For example, for a composite with perfectly aligned fibers χ_1 is 1, and if fibers are infinitely long, χ_2 is 1. It should be noted that the described model for tensile strength does not account for the fiber end effects and therefore overestimates the tensile strength.

Elastic moduli of discontinuous fiber composites can be calculated using the laminate analogy approach where the composite is simulated as sequential stacks of various laminae with different orientation and fiber lengths. The off-axis stress-strain relation for a laminate, $Q_{ij}^{'}$, can be used to find the laminate stiffness matrix for discontinuous fiber composites using:

$$\bar{A}_{ij} = \int_{l_{min}}^{l_{max}}\int_{\theta_{min}}^{\theta_{max}} Q_{ij}^{'}f(l)g(\theta)dld\theta \tag{7}$$

Finally, the composite tensile modulus is calculated using:

$$\bar{E}_{11} = \frac{\bar{A}_{11}\bar{A}_{22} - \bar{A}_{12}^2}{\bar{A}_{22}} \tag{8}$$

Elastic constants for unidirectional fiber composites were estimated from the Halpin-Tsai equations [31]. Finally, the fiber orientation coefficient, f_θ, was used to describe the average orientation of fibers in a specimen, where f_θ varies between −1 and 1, with −1 corresponding to fibers that are perpendicular to the measurement direction, 0 for random fiber orientation, and 1 corresponding to uni-axially aligned fibers along the loading direction:

$$f_\theta = \int_{\theta_{min}}^{\theta_{max}} g(\theta)\cos^2(\theta)d\theta - 1 \tag{9}$$

Input parameters to the models were experimentally measured or indirectly calculated using the Halpin-Tsai equations. The critical fiber length was estimated by fitting the strength equation to the strength values measured experimentally.

3. Results and discussions

3.1. Recycled fiber characterization

A representative scanning electron micrograph of recycled carbon fibers is shown in Fig. 5. The particles observed on the fiber surface are believed to be residual toughening particles from the original composite. Additionally, a small amount of residual epoxy and minor pitting can be observed on the fiber surface. SEM micrographs were also used to measure an average fiber diameter of 5.5 μm, while the reported diameter of virgin T800 carbon fibers is 5 μm [32]. Using the measured FLD and the average fiber diameter, the aspect ratio of the recycled fibers used in this study falls mostly within the 100–1000 range

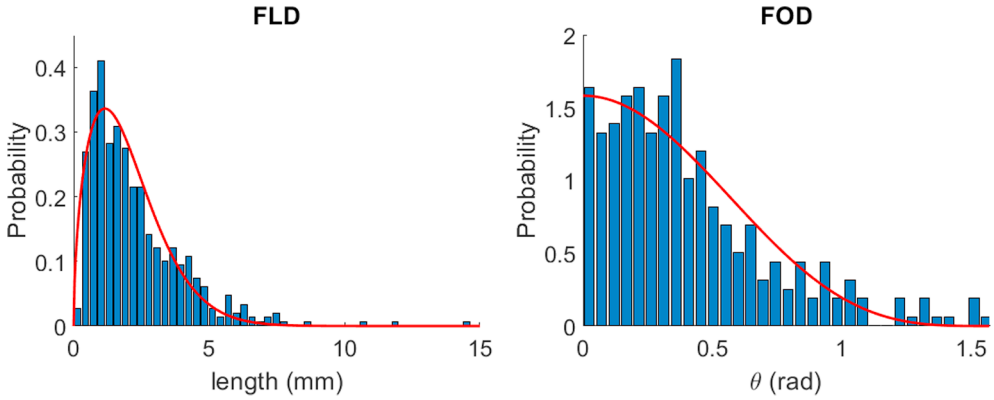

Fig. 4. Fiber length and orientation distributions (FLD and FOD, respectively) in a unidirectionally aligned sample and curve fits to them. (For interpretation of the references to colour in this figure legend, the reader is referred to the web version of this article.)

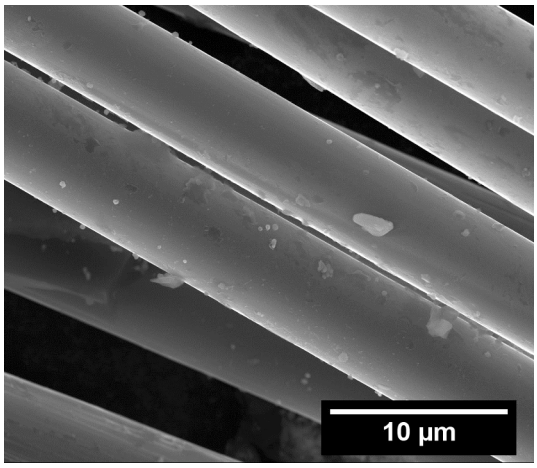

Fig. 5. SEM images of non-sized recycled carbon fibers.

(average aspect ratio of 300). Weibull analysis was used to find the scale parameter for the single fiber tensile test data, which was used as a measure of fiber strength. The fiber modulus was not affected by the recycling process. However, the strength experienced a 25.2% reduction compared with the virgin fibers.

The XPS results for recycled carbon fibers are summarized in Table 1; as recycled non-sized fibers, recycled and sized fibers, and recycled non-sized fibers that have been through the dispersion and alignment processing. The processed fibers were exposed to the water/glycerol solution, then rinsed with warm DI water to remove glycerol and dried above glycerol's boiling temperature for two hours. This data shows an increase in functional groups on the fiber surface due to sizing, however, the concentration of these groups changes upon processing. The relative percentage of O1s bonds increased from 12.1% to 18.5% due to the applied sizing. The C—OH and C—O bonds also increase from 59.8% to 74.3%, and 11.1% to 37.6%, from non-sized to sized fibers, respectively. These groups are available to bond to the amine groups of the epoxy and therefore are expected to increase the interfacial shear strength of the sized fibers [33–35]. Both C—OH and C—O bonds were significantly reduced after processing. There was an unusual increase in the concentration of amine groups on recycled fibers due to processing.

Table 1
XPS analysis of recycled carbon fiber surfaces.

	Non-sized	Sized	Processed non-sized
C═C	61.6%	34.6%	56.4%
O1s	12.1%	18.5%	15.0%
C—OH	59.8%	74.3%	54.1%
C—O	11.1%	37.6%	13.3%
Amine	25.5%	32.2%	63.2%
O/C ratio	14.3%	23.2%	18.7%

3.2. Recycled carbon fiber composite characterization

The aligned and non-aligned fiber mats were characterized with optical microscopy, as shown in Fig. 6. The aligned virgin fiber tow demonstrates the maximum packing efficiency of the fibers. While substantial alignment can be observed in the aligned recycled fiber mat, the misaligned fibers can be seen to limit the packing efficiency.

Micrographs of the composite cross-sections taken using a light microscope are shown in Fig. 7. Virtually no voids from the composite manufacturing were observed in the composites. Highly misaligned fibers can be observed in both the aligned and non-aligned composites, though of course are more prevalent in the randomly oriented composite. It can also be observed that the fibers in both samples are almost perfectly aligned in the plane direction, i.e., no misaligned fiber in the through-the-thickness (horizontal) direction. The fiber packing density also is higher in the aligned fiber composite. The highly misaligned fibers result in a substantial decrease in the ability of fibers to pack efficiently together, resulting in low volume fractions.

The data collected from micro-computed tomography (μCT) is shown in Fig. 8. Again, misaligned fibers can be observed within the matrix. It is also evident that a substantial amount of contamination is present within the composite, as illustrated by the contrasting phases illustrated. While some of these phases have a fiber morphology, the exact composition of these contaminants is not known. It is likely that contaminants will act as defects in the matrix, potentially reducing the mechanical properties of the composites.

SEM micrographs of the fractured surfaces can be observed in Fig. 9. Substantial fiber pullout, along with the clean surface of the fibers, suggests low interfacial bond strength between the fibers and the matrix. This property is observed across the recycled fibers that were non-sized, sized, and sized and heated to 300 °C. Virgin chopped fibers were also processed into mats and subsequently composite plates were fabricated; following identical protocol used for recycled fibers. Fractography of these specimens also suggested a low interfacial strength evident by the pulled-out clean fiber surfaces. This result suggests that processing the fibers in water and glycerol adversely affects the ability of the surface to form covalent bonds with the epoxy matrix. These findings agree with the carbon fiber surface activities measured via XPS, suggesting that the processing significantly reduces some of the functional groups on carbon fiber surface.

The mechanical properties of the rCF composites are tabulated in Table 2. A minimum of five coupons were tested for each configuration. The first two rows summarize properties for the non-aligned composites

Fig. 6. Aligned virgin fiber (left), non-aligned recycled fiber (middle) and aligned recycled fiber (right). (For interpretation of the references to colour in this figure legend, the reader is referred to the web version of this article.)

and the last three rows are for aligned composites. It was difficult to maximize the volume fraction beyond the obtained range of 18–24%; higher volume fractions can be obtained by using higher molding pressures. However, higher molding pressures can also lead to fiber breakage and lower average fiber lengths. FLD and FOD for the aligned rCF composites was used in the model to extract the tensile properties, as shown in the last row. While the model predicts the modulus well, a weak interfacial strength was used to match the experimental strength values. As such, the critical fiber length was calculated to be 4 mm; the critical fiber length is inversely proportional to the interfacial bond strength between the fiber and matrix. The estimated value of 4 mm is an order of magnitude higher than that reported for carbon fiber-epoxy systems [36], highlighting the poor interfacial bond between the carbon fibers used in this study with the epoxy matrix. Composites based on virgin fibers also showed similar strength values confirming that the weak interfaces are a result of the processing approach used here. As mentioned earlier, the model overestimates strength values because it does not account for fiber end effects. The μCT also revealed impurities in the composite. The presence of impurities, weak fiber-matrix interfacial bonding, and fiber end effects collectively contribute to the relatively low strength of the rCFRP samples. The mechanical properties of the non-aligned composites highlight the importance of fiber alignment on both the modulus and strength in rCF reinforced composites. The effect of alignment can also be understood by comparing the

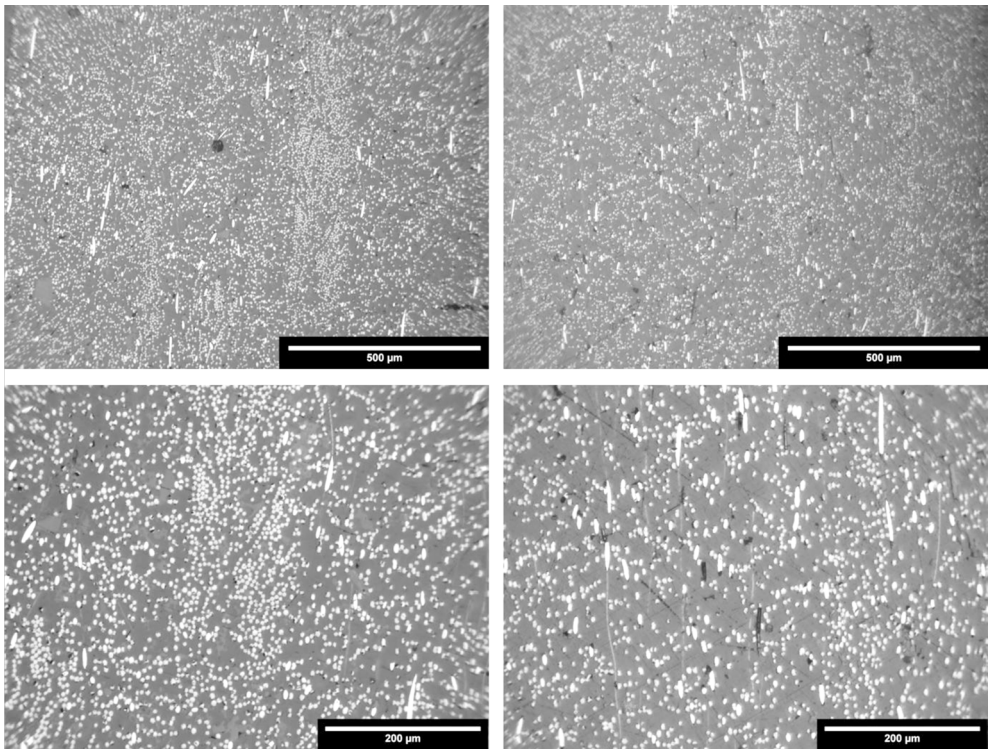

Fig. 7. Through-the-thickness cross-sectional micrographs of recycled carbon fiber composites. 10× (top) and 20× (bottom) magnification images are shown of an aligned (left) and randomly oriented (right) rCF composites. White and back areas are fibers and voids, respectively, and the grey background represents the polymer matrix. The cross-section of the aligned sample is perpendicular to the fiber alignment direction, while the cross-section of the randomly oriented sample was chosen arbitrarily. Cross-section of perfectly aligned fibers is complete circles while misaligned fibers are seen as ellipses, where the length of the major ellipse axis is proportional to the fiber misalignment degree. For all the images, the sample thickness is in the horizontal direction.

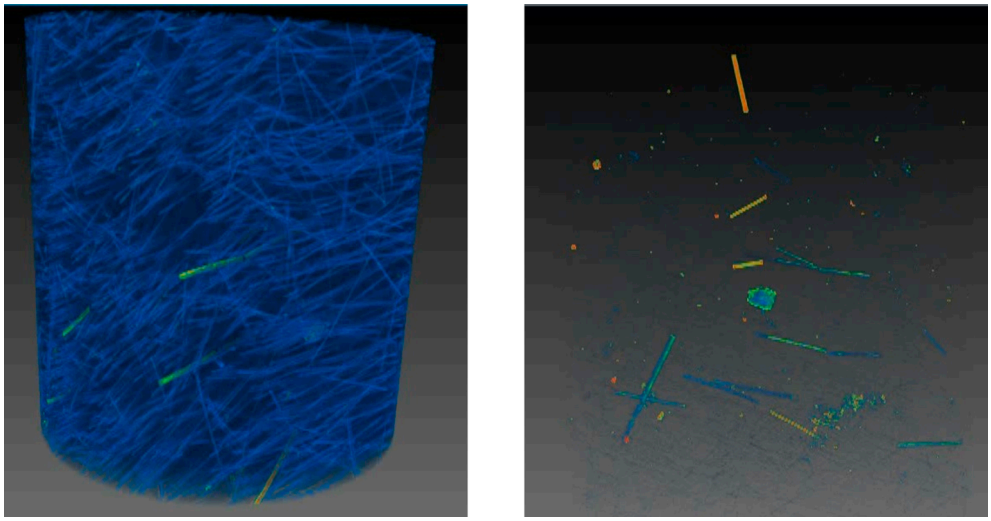

Fig. 8. Micro computed tomography (μCT) generated image of the recycled carbon fiber composite (left) and contaminates within the composite (right). (For interpretation of the references to colour in this figure legend, the reader is referred to the web version of this article.)

aligned, sized samples with the non-aligned, sized sample. If these strength and modulus values are normalized to the volume fraction of the composite, isolating the influence of alignment, the strength and modulus are improved by 100.0% and 136.7%, respectively. Again, normalizing the properties to the volume fractions, the addition of a sizing agent resulted in an increase in the strength by 3.9%, but a reduction in the modulus by 20.0%. It is, therefore, concluded that sizing did not have a strong effect on the tensile strength in aligned samples.

A comparison of these composite properties to those of continuous

Table 2
Tensile strength and modulus of recycled carbon fiber composites.

Sizing	Alignment	v_f	Strength (MPa)	Modulus (GPa)
Yes	No	20	93 ± 9.5	11. ± 0.7
Virgin fiber	No	20	104 ± 3.6	1 ± 0.7
No	Yes	18	192 ± 23.1	31.6 ± 0.9
Yes	Yes	24	266 ± 28.2	33.7 ± 2.2
Model	Yes	20	325	33.8

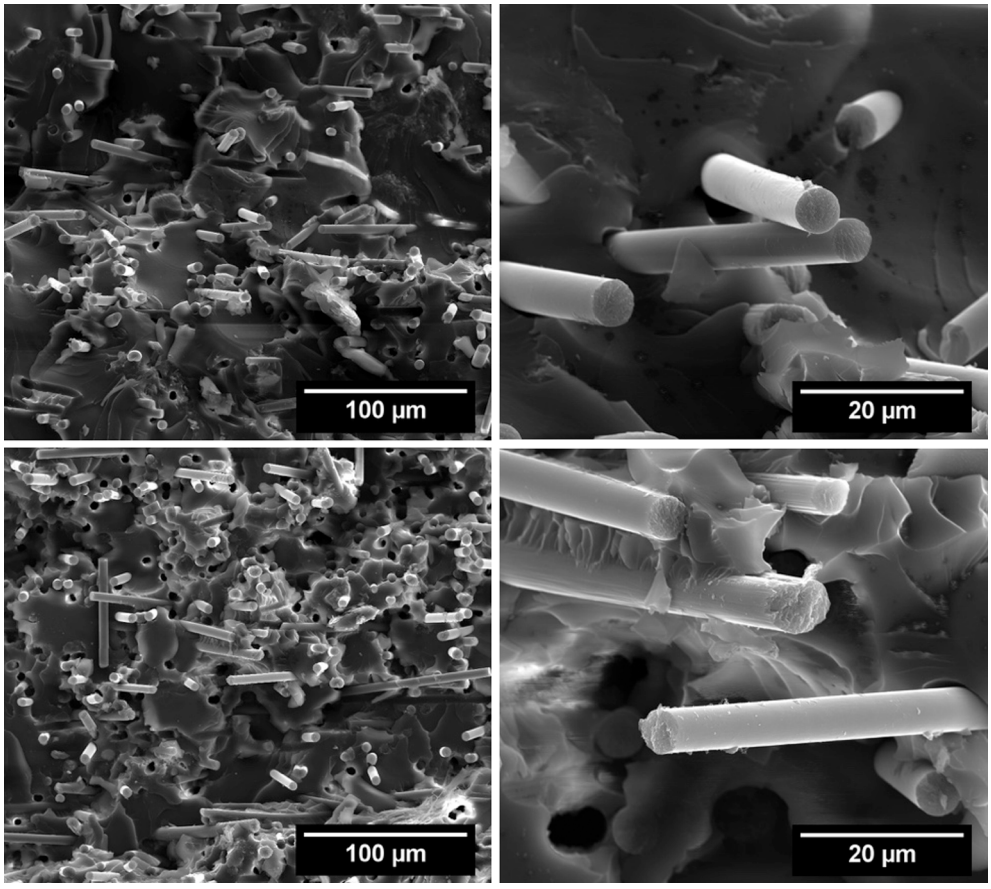

Fig. 9. SEM of recycled carbon fiber composite fractured surface for non-sized (top) and sized (bottom) samples.

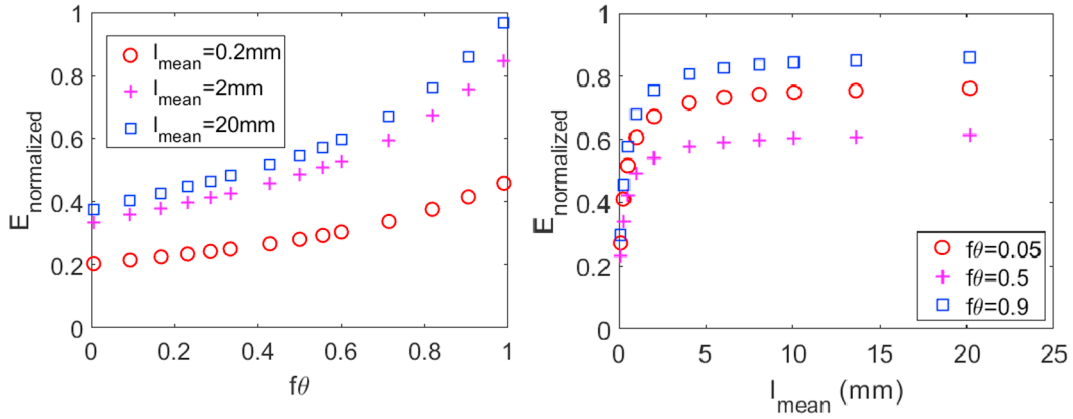

Fig. 10. left: Normalized Young's modulus as a function of fiber alignment. right: Normalized Young's modulus as a function of mean fiber length (mm). $f_\theta = 0$ corresponds to randomly aligned fibers, while $f_\theta = 1$ corresponds to perfectly aligned fibers. (For interpretation of the references to colour in this figure legend, the reader is referred to the web version of this article.)

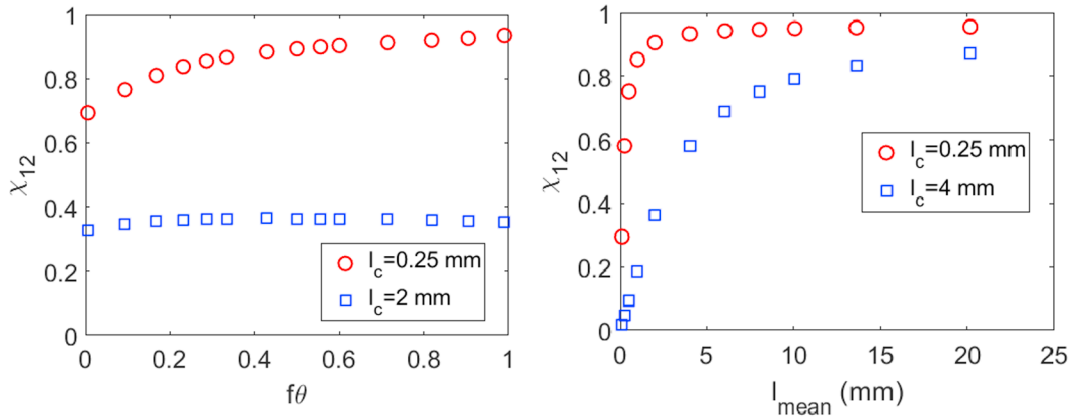

Fig. 11. left: Composite strength as a function of fiber orientation for two values of critical length. right: χ_{12} as a function of mean fiber length (mm) for two given critical lengths. $f_\theta = 0$ corresponds to randomly aligned fibers, while $f_\theta = 1$ corresponds to perfectly aligned fibers. (For interpretation of the references to colour in this figure legend, the reader is referred to the web version of this article.)

virgin fiber composites can be a valuable metric to gauge the effectiveness of the recycled fiber composites. Unidirectional virgin T800 composites with a 60% volume fraction have a tensile strength and modulus of 2650 MPa and 170 GPa, respectively [32]. With this metric, the translation efficiency of the aligned, sized recycled fiber composite for strength and modulus is 10% and 20%, respectively. This gauge considers the effects of change in length, surface quality, and volume fraction that accompanies the recycling and remanufacturing processes. As the recycled fibers can be an order of magnitude cheaper compared with the virgin T800 fibers, a composite approaching virgin fiber property is not necessary to be competitive in the market but improving the translation efficiency will be necessary to see the incorporation of recycled fibers into high-volume markets.

3.3. Recycled fiber composite modeling

Using the model detailed in Section 2.9, the relationship between the normalized composite modulus and fiber orientation angle is plotted in Fig. 10. Young's modulus values were normalized to the modulus of a composite with continuous, perfectly aligned fibers at 20% fiber volume fraction. The shape of the observed length distribution was used in this model, but the average length was varied when shown. The intention of this model is to understand the influence of multiple parameters on composite properties in order to identify the highest value methods of improving composite properties. As expected, as the fibers become more aligned along the tensile axis, the composite modulus monotonically increases. The trend observed in this plot is not linear, which illustrates the importance of increasing the fiber orientation above an f_θ of 0.7. The relationship between normalized modulus and mean fiber length (fiber diameter was 5.5 μm) is shown in Fig. 10. Again, the intuitive trend of increasing modulus with increasing mean fiber length is observed. The figure demonstrates the importance of maintaining a mean fiber length at the millimeter scale. For both weakly and strongly aligned fibers, the normalized modulus is significantly reduced below 5 mm mean lengths. Increasing the mean fiber length above 5 mm does not produce a significant increase in the composite modulus. Therefore, it appears necessary to maintain a mean fiber length of 2–3 mm to produce composites with a competitive modulus, which is independent of the fiber critical length. Therefore, maintaining a minimum mean fiber length of 2 mm while achieving an f_θ of greater than 0.7–0.8 will be necessary for producing high modulus composites. It should also be noted that higher volume fractions can be achieved when fibers are more aligned. If fibers are not highly aligned in the mat, composite specimens can be fabricated under high molding pressures at the price of shortening and damaging the fibers.

The parameter χ_{12} can be used to predict the composite strength. χ_{12} varies between 0 and 1, with 1 representing the maximum achievable composite strength with continuous fibers. The relationship between χ_{12} and f_θ is illustrated in Fig. 11. For a long critical fiber length (4 mm), there does not appear to be a dependence of composite strength on fiber orientation. However, at low critical lengths (0.25 mm), fiber alignment does increase the strength of the composite. However, the incremental increase in strength is diminished above an f_θ of 0.5, at which point the composite can be expected to achieve a strength near the optimum

value. It can be concluded that the critical fiber length significantly influences the strength of composite while fiber orientation has a lower influence on the strength. This is contrary to the composite elastic modulus dependence on orientation where there exists a strong relationship.

The dependence of composite strength on mean fiber length was further explored in Fig. 11. For a low critical fiber length (0.25 mm), the strength reaches a plateau at a fiber length of only a few millimeters. Above 5 mm, only slight improvements of the strength can be observed. At high critical fiber lengths, however, increasing the mean fiber length continues to produce improvements in strength up to centimeter scale mean fiber lengths. This indicates that strength can be maximized at low mean fiber lengths when the critical length is small, while long fibers are necessary to increase the strength for relatively long critical fiber lengths.

In general, the strength of the tested composites also falls short of predicted values. This may be the result of weak interfacial shear strength, resulting in a long critical fiber length, combined with a low average fiber length, and the fiber end effects that are not accounted for in the model. Therefore, a longer average fiber length and lower critical length are required to achieve a high-performance recycled carbon fiber composite. Additionally, an increase in the degree of fiber alignment would also result in an increased composite tensile modulus. In summary, f_{θ} and l_{mean} above 0.7 and 5 mm, respectively, can be expected to produce a high modulus composite. Similarly, a mean fiber length above 3 mm is expected to produce a high strength composite for short critical lengths (e.g., $l_c = 0.25$), while a mean fiber length above 10 mm is required for longer critical lengths (e.g., $l_c = 4$ mm). The fiber ends only partially carry loads and cause stress concentrations in adjacent fibers. Recycling technologies as well as the difficulty in dispersing and aligning long fibers limit the maximum fiber length achievable in rCFRPs. This complex problem calls for multi-objective optimization of mechanical properties with respect to feasible FLD, FOD, and volume fractions.

4. Conclusions

The effect of alignment and sizing of recycled carbon fiber composites was investigated experimentally and analytically. Randomly oriented 2D carbon fiber mats were manufactured through a dispersion and filtration method. Aligned carbon fiber mats were fabricated using a similar dispersion process coupled with a centrifugal alignment rig. Analysis of SEM micrographs did not show any substantial degradation or contamination on the fiber surface after the sizing process. XPS did show an increase in active chemical groups on the fiber surface after sizing, which are known to bond with the epoxy used in this study. Processing of sized fibers in glycerol and water, degraded surface functionality of fibers, resulting in weak bonding to the epoxy used in this study. Image analysis found that the alignment process could produce mats with roughly 70% of fibers aligned within ± 15° of the mean direction. The effect of processing on the average fiber length was also evaluated, finding that the average fiber length after processing was roughly 1.5 mm.

The degree of alignment was unsurprisingly found to have the largest influence on the strength and elastic modulus of the composites. The aligned composite had an increase in normalized tensile strength and modulus of 100% and 137%, respectively, over the non-aligned composite. Sizing did not have a strong effect on properties. This could have been due to the deteriorating effects of glycerol/water processing on carbon fiber surfaces. Further improving the alignment will allow for an enhanced composite volume fraction, which is necessary to realize improvements in the translation efficiency of recycled fiber composites beyond 10–20%.

To put the findings of this paper in perspective, one should consider the price and properties of non-carbon fiber types. For example, the recycled T800 fibers used here possess a similar strength to S-glass fibers, however, are almost four times stiffer (elastic modulus) and less expensive; price of recycled carbon fibers is predicted to be lower than S-glass. For high performance applications, unidirectional S-glass fiber composites (volume fraction of 50%) achieve better strength and similar elastic modulus compared with recycled carbon fiber composites (aligned and 15–20% volume fraction). For several applications, such as injection molded parts and 3D printed composites [37], short fibers at relatively low (< 20%) volume fractions are employed. In such applications, the combination of the high modulus and low cost of the recycled fibers is unrivaled. It should finally be noted that carbon fibers impart other functionalities such as low thermal expansion and electrical conductivity that might be critical for some applications.

An analytical model was used to examine the significance of fiber length and orientation. The model indicated that low fiber lengths relative to the critical length could dramatically reduce the strength and modulus of the composites. This result suggests that further effort may be needed to retain relatively long fibers during the recycling as well as the dispersion and alignment processes. Ideally, fibers longer than 5 mm in length can be expected to produce composites with exceptional strength and elastic modulus. Additionally, a low critical fiber length is necessary to improve the strength of the composites. Finally, improving fiber alignment improves the composite's elastic modulus and fiber volume fraction, though the improvement in composite strength is likely to be influenced to a lesser extent.

5. Declarations of interest

None.

Acknowledgements

The authors would like to acknowledge the National Science Foundation, award #1544084, whose funding made this research possible. Additionally, the authors would like to thank Adherent Technologies Inc. for providing the recycled carbon fibers.

References

[1] Tehrani M, Boroujeni AY, Hartman TB, Haugh TP, Case SW, Al-Haik MS. Mechanical characterization and impact damage assessment of a woven carbon fiber reinforced carbon nanotube-epoxy composite. Compos Sci Technol 2013;75:42–8.
[2] Das S, Warren J, West D, Schexnayder SM. Global carbon fiber composites supply chain competitiveness analysis. Technical report ORNL/SR-2016/100 | NREL/TP-6A50-66071; 2016. p. 1–116.
[3] Wood K. Carbon fiber reclamation: going commercial. High Perform Compos 2010;3:p1–2.
[4] Pimenta S, Pinho ST. Recycling carbon fibre reinforced polymers for structural applications: technology review and market outlook. Waste Manage 2011;31(2):378–92.
[5] Carberry W. Airplane recycling efforts benefit Boeing operators. Boeing AERO Magazine QRT 2008;4(08):6–13.
[6] Campbell FC. Structural composite materials. ASM International; 2010.
[7] Witik RA, Teuscher R, Michaud V, Ludwig C, Manson JAE. Carbon fibre reinforced composite waste: an environmental assessment of recycling, energy recovery and landfilling. Compos Part a-Appl S 2013;49:89–99.
[8] Pang EJX, Chan A, Pickering SJ. Thermoelectrical properties of intercalated recycled carbon fibre composite. Compos Part a-Appl S 2011;42(10):1406–11.
[9] Pickering S, Kelly R, Kennerley J, Rudd C, Fenwick N. A fluidised-bed process for the recovery of glass fibres from scrap thermoset composites. Compos Sci Technol 2000;60(4):509–23.
[10] Nahil MA, Williams PT. Recycling of carbon fibre reinforced polymeric waste for the production of activated carbon fibres. J Anal Appl Pyrol 2011;91(1):67–75.
[11] Jiang GZ, Pickering SJ. Recycled carbon fibres: contact angles and interfacial bonding with thermoset resins. Mater Sci Forum 2012;714:255–61.
[12] Jiang GZ, Pickering SJ. Structure-property relationship of recycled carbon fibres revealed by pyrolysis recycling process. J Mater Sci 2016;51(4):1949–58.
[13] Pickering SJ. Recycling technologies for thermoset composite materials - current status. Compos Part a-Appl S 2006;37(8):1206–15.
[14] Pinero-Hernanz R, Dodds C, Hyde J, Garcia-Serna J, Poliakoff M, Lester E, et al. Chemical recycling of carbon fibre reinforced composites in nearcritical and supercritical water. Compos Part a-Appl S 2008;39(3):454–61.
[15] Jiang G, Pickering SJ, Lester EH, Turner TA, Wong KH, Warrior NA. Characterisation of carbon fibres recycled from carbon fibre/epoxy resin

composites using supercritical n-propanol. Compos Sci Technol 2009;69(2):192–8.
[16] Matthew Such CW, Potter Kevin. Aligned Discontinuous fibre composites: a short history. J Multifunct Compos 2014;3:155–68.
[17] Turner TA, Warrior NA, Pickering SJ. Development of high value moulding compounds from recycled carbon fibres. Plast Rubber Compos 2010;39(3–5):151–6.
[18] Yu H, Potter KD, Wisnom MR. A novel manufacturing method for aligned discontinuous fibre composites (high performance-discontinuous fibre method). Compos Part a-Appl S 2014;65:175–85.
[19] Allred RE, Gosau JM, Shoemaker JM. Recycling process for carbon/epoxy composites. In: 46th International SAMPE symposium and exhibition. Long Beach, CA2001. p. 179–92.
[20] Allred RE, Doak TJ, Busselle LD, Gordon BW, Harrah LA, Hoyt AE. Catalytic conversion process for recycling navy shipboard plastic wastes. Polym Mater Sci Eng 1997;76:579-.
[21] Boroujeni AY, Tehrani M, Nelson AJ, Al-Haik M. Effect of carbon nanotubes growth topology on the mechanical behavior of hybrid carbon nanotube/carbon fiber polymer composites. Polym Compos 2016;37(9):2639–48.
[22] Tehrani M, Boroujeni AY, Luhrs C, Phillips J, Al-Haik MS. Hybrid composites based on carbon fiber/carbon nanofilament reinforcement. Materials 2014;7(6):4182–95.
[23] Weibull W. A statistical distribution function of wide applicability. J Appl Mech-T ASME 1951;18(3):293–7.
[24] Wong KH, Turner TA, Pickering SJ, Warrior NA. The potential for fibre alignment in the manufacture of polymer composites from recycled carbon fibre. SAE Int J Aerospace 2009;2(2009-01-3237):225–31.
[25] Fu S-Y, Lauke B. Effects of fiber length and fiber orientation distributions on the tensile strength of short-fiber-reinforced polymers. Compos Sci Technol 1996;56(10):1179–90.
[26] Garoushi S, Lassila L, Vallittu P. Short fiber reinforced composite: the effect of fiber length and volume fraction. J Contemp Dent Pract 2006;7(5):10–7.
[27] Fu YS, Lauke B. The elastic modulus of misaligned short-fiber-reinforced polymers. Compos Sci Technol 1998;58(3):389–400.
[28] Jayaraman K, Kortschot MT. Correction to the Fukuda-Kawata Young's modulus theory and the Fukuda-Chou strength theory for short fibre-reinforced composite materials. J Mater Sci 1996;31(8):2059–64.
[29] Piggott MR. Short fibre polymer composites: a fracture-based theory of fibre reinforcement. J Compos Mater 1994;28(7):588–606.
[30] Fu SY, Lauke B, Mai YW. Science and engineering of short fibre reinforced polymer composites. Sci Eng Short Fibre Reinforced Polym Compos 2009. p. 1–338.
[31] Halpin JC, Tsai SW. Environmental factors in composite materials design. US Air Force Materials Lab. Rep. AFML Tech Rep; 1967. p. 67–423.
[32] Toray Carbon Fibers America I. Technical Data Sheet No. CFA-007.
[33] Tang LG, Kardos JL. A review of methods for improving the interfacial adhesion between carbon fiber and polymer matrix. Polym Compos 1997;18(1):100–13.
[34] Dai ZS, Shi FH, Zhang BY, Li M, Zhang ZG. Effect of sizing on carbon fiber surface properties and fibers/epoxy interfacial adhesion. Appl Surf Sci 2011;257(15):6980–5.
[35] Weitzsacker CL, Xie M, Drzal LT. Using XPS to investigate fiber matrix chemical interactions in carbon-fiber-reinforced composites. Surf Interface Anal 1997;25(2):53–63.
[36] Herrerafranco PJ, Drzal LT. Comparison of methods for the measurement of fiber matrix adhesion in composites. Composites 1992;23(1):2–27.
[37] Werken Nd, Hurley J, Khanbolouki Pouria, Sarvestani AN, Tamijani AY, Tehrani Mehran. Design considerations and modeling of fiber reinforced 3D printed parts. Compos B Eng 2018;160:684–92.